

**NASA  
Technical  
Paper  
2797**

1988

# A Simplified Approach to Axisymmetric Dual-Reflector Antenna Design

Raymond L. Barger

*Langley Research Center  
Hampton, Virginia*

**NASA**

National Aeronautics  
and Space Administration

Scientific and Technical  
Information Division

## Summary

A procedure is described for designing dual-reflector antennas. The analysis is developed by taking each reflector to be the envelope of its tangent planes. The slopes of the emitted rays are specified rather than the phase distribution in the emitted beam. Thus, both the output wave shape and the angular distribution of intensity can be specified.

Computed examples include variations from both Cassegrain and Gregorian systems. These examples include deviation from uniform source distributions and from the parallel-beam property of conventional systems.

## Introduction

In theory it is possible to specify, within limits, both the emitted amplitude distribution and the phase distribution of a dual-reflector system when both surfaces are properly shaped. The problem of determining these shapes has been treated in references 1 and 2 with a combination of differential and algebraic equations. This system of equations tends to be unwieldy, and consequently in both references the method of solution is only indicated, with the specific formulas omitted.

Although the present approach is an approximate procedure, it can, in theory, be made as accurate as desired by taking sufficiently small step sizes. The simplifying concept is to treat each of the two reflectors as the envelope of its tangent planes. This technique permits the mathematical problem to be reduced to one of solving a set of nonlinear algebraic equations.

Computed examples include both modified Cassegrain and modified Gregorian systems. Inasmuch as the emphasis in the present analysis is on simplicity of concept, only axisymmetric systems are treated. It should be noted that if the reflector system utilizes only a segment (e.g., a quadrant) of the axisymmetric design, then a cross polarization exists in the output beam since the antenna normally does not emit a circularly polarized wave.

## Symbols

$b$	exponent of $\cos \theta_0$
$E$	beam energy
$I$	intensity
$m$	slope of ray relative to system centerline
$R$	$\equiv \frac{-2m_2}{m_2^2 - 1}$

$x, y$	coordinates, $x$ taken along system centerline and $y$ in radial direction
$(X_1, Y_1), (X_2, Y_2)$	midpoint of straight segment tangent to reflector meridian line
$X_3, Y_3$	point at which ray intersects reference plane
$(x_1, y_1), (x_2, y_2)$	initial point of straight segment tangent to reflector meridian line
$\theta$	angle ray makes with system centerline
Subscripts:	
0	origin or ray emanating from origin
1	tangent segment of subreflector
2	tangent segment of main reflector
3	vertical plane along which output intensity is specified
$b$	ray reflected from main reflector
$c$	ray reflected from subreflector to main reflector
$i$	index
min, max, total	minimum, maximum, and total

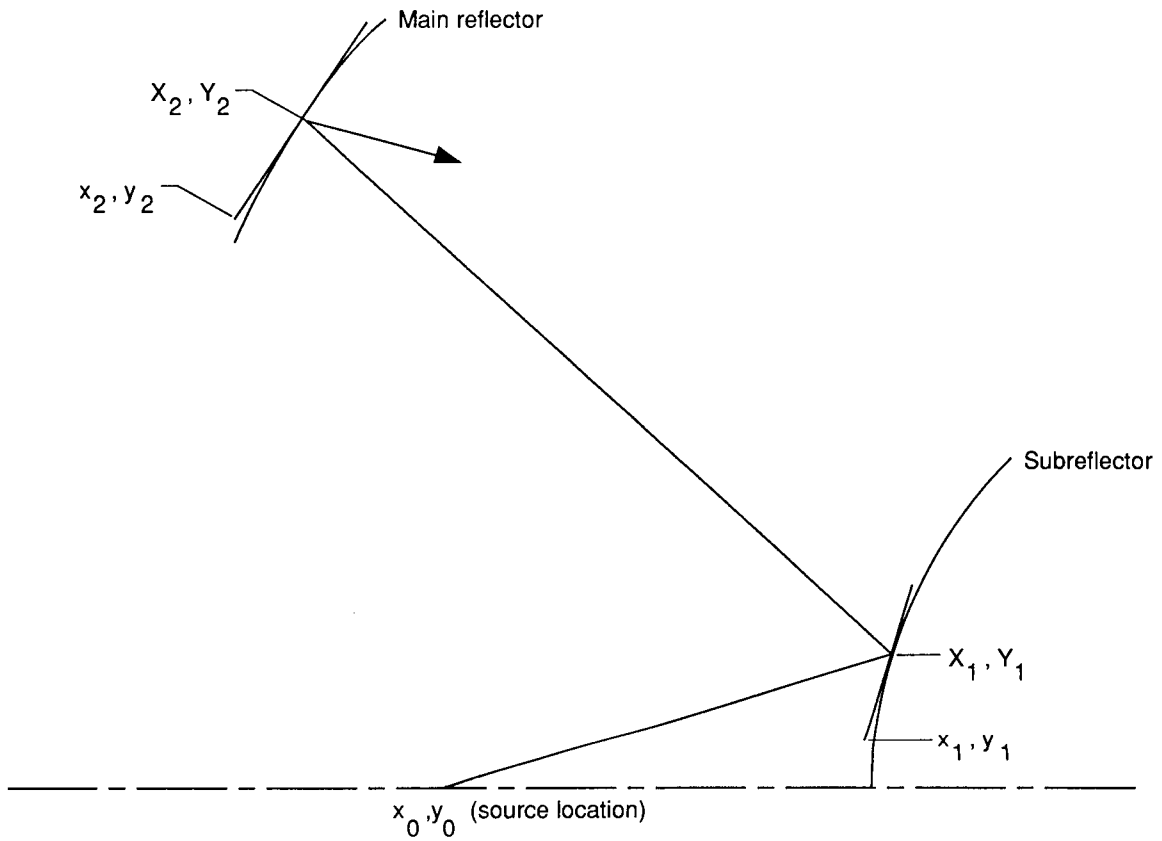
## Analysis

### Reflector and Ray Geometry

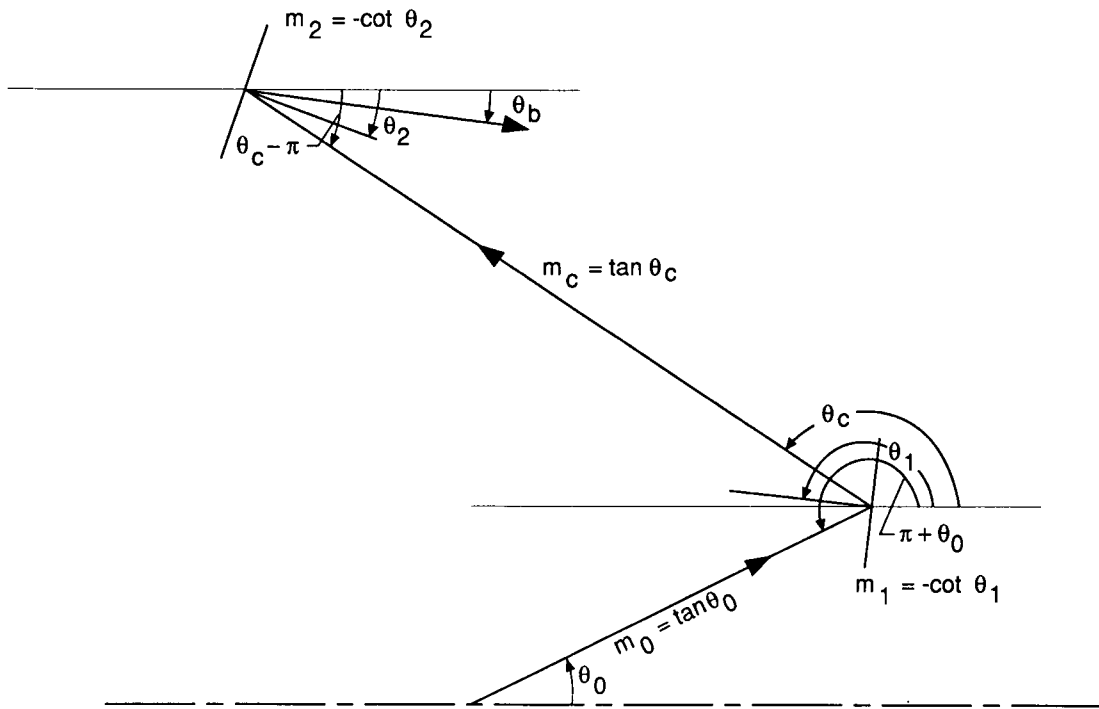
As was mentioned in the *Introduction*, each curved reflector surface is treated as the envelope of its tangent planes. Since each of these surfaces is axisymmetric, it can be specified by the meridian line cut by a vertical plane. Then the tangent plane along this meridian appears simply as a straight line segment. (See fig. 1(a).)

The geometry for tracing a ray through the system is shown in figure 1(b). The reflection condition at the subreflector gives

$$2\theta_1 = \theta_c + (\pi + \theta_0) \quad (1)$$



(a) Tangent-plane geometry.



(b) Angles and slopes.

Figure 1. Basic system geometry.

To find the relation between the slopes, we take the tangent of both sides:

$$\tan 2\theta_1 = \frac{2 \tan \theta_1}{1 - \tan^2 \theta_1} = \frac{\tan \theta_c + \tan \theta_0}{1 - \tan \theta_c \tan \theta_0} \quad (2)$$

Similarly, at the second reflector,

$$\tan(2\theta_2) = \tan[\theta_3 + (\theta_c - \pi)] \quad (3)$$

or

$$\frac{2 \tan \theta_2}{1 - \tan^2 \theta_2} = \frac{\tan \theta_3 + \tan \theta_c}{1 - \tan \theta_3 \tan \theta_c} \quad (4)$$

Since the slope of the local tangent to the reflector is the negative reciprocal of the slope of its normal ( $m_1 = -\cot \theta_1$ ), equation (2) yields

$$\frac{-2m_1}{m_1^2 - 1} = \frac{m_0 + m_c}{1 - m_0 m_c} \quad (5)$$

and, similarly, equation (4) yields

$$\frac{-2m_2}{m_2^2 - 1} = \frac{m_3 + m_c}{1 - m_3 m_c} \quad (6)$$

Referring to figure 1(a), if we denote the coordinates of the initial point of a subreflector segment by  $(x_1, y_1)$  and denote the reflection points by capital letters  $(X_1, Y_1)$ , then the reflection point is specified to be at the midpoint of the segment simply by taking the segment length to be twice the distance from  $(x_1, y_1)$  to  $(X_1, Y_1)$ . The main reflector is treated similarly. The slopes and point coordinates are related linearly as follows:

$$m_c = \frac{Y_2 - Y_1}{X_2 - X_1} \quad (7)$$

$$m_0 = \frac{Y_1 - y_0}{X_1 - x_0} \quad (8)$$

$$m_1 = \frac{Y_1 - y_1}{X_1 - x_1} \quad (9)$$

$$m_2 = \frac{Y_2 - y_2}{X_2 - x_2} \quad (10)$$

The intensity distributions are determined as follows. The intensity distribution to be assigned arbitrarily as the output of the system is most conveniently specified along a vertical plane, usually taken near the aperture plane. Thus, if the output intensity distribution  $I(Y_3)$  is assigned as a function of  $Y_3$  along a vertical plane taken at  $X_3$ , then the ray that intersects this plane at  $Y_3$  is related to the initial source emission angle  $\theta_0$  through the energy relation, which is given in the next section. Furthermore,

it is appropriate, with the present method, to specify the ray slope distribution of the system output beam rather than the phase distribution. Thus (see fig. 2(a)), in the equation for the ray reflected from  $(X_2, Y_2)$  through  $(X_3, Y_3)$ ,

$$m_b = \frac{Y_3 - Y_2}{X_3 - X_2} \quad (11)$$

and  $X_3$ ,  $Y_3$ , and  $m_b$  are all known quantities.

### Energy Relation

The value of  $Y_3$  is determined from the energy relation as follows. The intensity distribution  $I_0(\theta_0)$  emitted by the source antenna is (see fig. 2(b))

$$2\pi I_0(\theta_0) \sin \theta_0 \, d\theta_0$$

and consequently all the energy emitted within this segment is

$$E_0(\theta_0) = 2\pi \int_{\theta_{\min}}^{\theta_0} I_0(\theta) \sin \theta \, d\theta \quad (12)$$

and the relative amount of energy emitted is

$$\frac{E_0(\theta_0)}{E_0(\theta_{0,\max})} = \frac{E_0(\theta_0)}{E_{\text{total}}} \quad (13)$$

where  $\theta_{0,\max}$  denotes the edge of that part of the source beam that is to be utilized.

The intensity of the output beam is specified as a function of  $Y_3$  along the vertical plane at  $X_3$ . Thus, the energy emitted through the annulus at  $Y_3$  with width  $dY_3$  is (see fig. 2(a))

$$2\pi I_3(Y_3) Y_3 \, dY_3$$

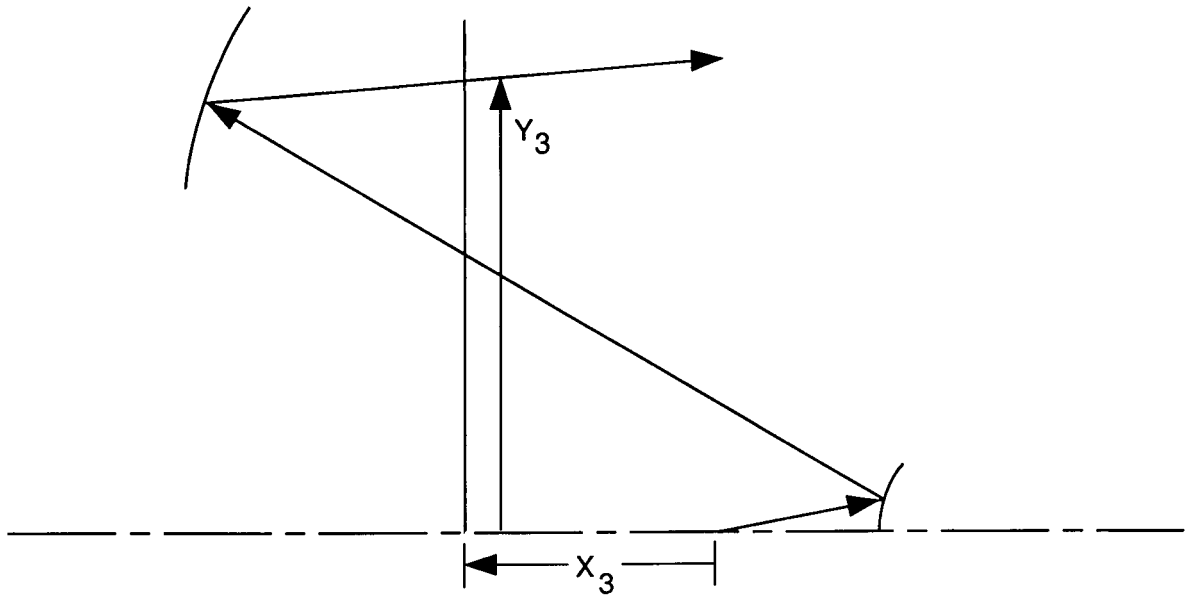
The energy emitted through the ring at  $Y_3$  is

$$E(Y_3) = 2\pi \int_{Y_{3,\min}}^{Y_3} I_3(y) y \, dy \quad (14)$$

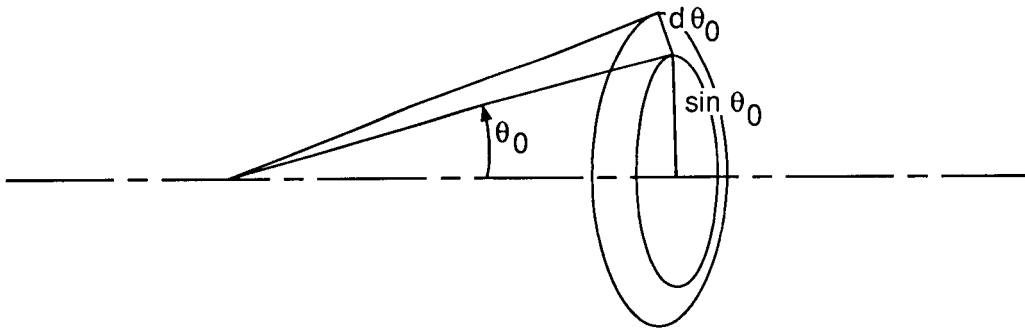
where the ray through  $Y_{3,\min}$  is that emitted at  $\theta_{0,\min}$  by the source. The relative energy is

$$\frac{E(Y_3)}{E(Y_{3,\max})} = \frac{E(Y_3)}{E_{\text{total}}} \quad (15)$$

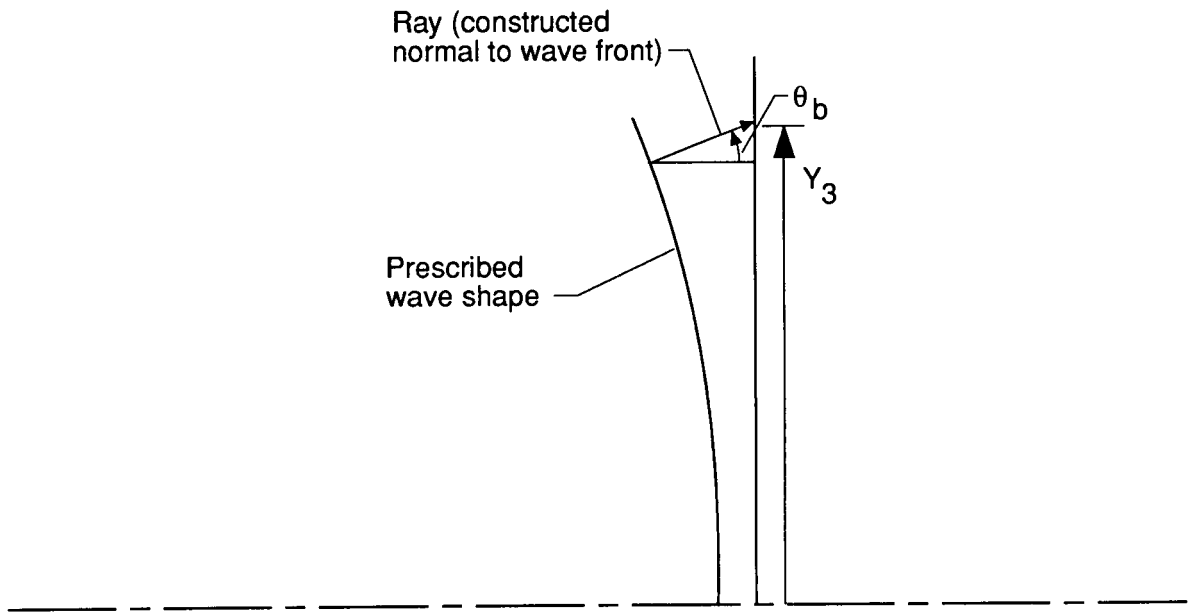
Comparing equation (15) with equation (13) enables one to determine the  $Y_3$  corresponding to a given  $\theta_0$ . As a rule, the prescribed intensity distribution  $I_3(y)$  in equation (14) is taken as a relatively simple analytic expression. Consequently, the energy integral



(a) Vertical reference plane at  $X_3$ .



(b) Source rays at unit circle.



(c) Method for determining  $Y_3$  and  $\theta_b$  from prescribed wave shape.

Figure 2. Geometry for identifying source ray at  $\theta_0$  with emitted ray through  $(X_3, Y_3)$ .

in equation (14) can be evaluated in closed form and  $E(Y_3)$  is determined in analytic form. Furthermore, the source intensity distribution  $I_0(\theta)$  can often be described as some power of  $\cos \theta$  or as a linear combination of such functions, so that  $E(\theta_0)$  can be determined in analytic form from equation (12).

Before proceeding to the solution of the equations for the reflector surfaces, we may pursue further the significance of the form of the system performance specification. Although for some problems it is appropriate to specify the intensity and beam direction distributions along some vertical plane, it is important to observe that these distributions can be obtained by specifying the more fundamental quantities of output wave shape and the intensity distribution as a function of ray direction. Thus, in reference to figure 2(c), the wave shape and the relative energy as a function of  $\theta_b$  are prescribed. Since the wave shape is known, normals to the wave shape can be constructed and their intersections with the vertical plane at  $X_3$  determined. These normals, which represent rays, have slope  $m_b = \tan \theta_b$ . Thus, with  $E(\theta_b)$  prescribed, these intersections determine  $E(Y_3)$ . Consequently, both  $m_b$  and  $Y_3$  are determined for each ray of the output beam.

### Solution of Equations

To determine the reflector shapes, the set of seven equations (5) to (11) are to be solved for the unknown quantities  $X_1, Y_1, X_2, Y_2, m_1, m_2$ , and  $m_c$ . The approach taken here is to eliminate all unknowns except  $m_2$ , solve the resulting (highly nonlinear) equation for  $m_2$  numerically, and then substitute back into the other equations to determine the remaining unknowns. The details of this procedure follow.

Define

$$R(m_2) \equiv \frac{-2m_2}{m_2^2 - 1} \quad (16)$$

and substitute  $R$  into equation (6), which (noting that  $m_3 = m_b$ ) can then be written as

$$(1 - m_b m_c)R(m_2) = m_b + m_c$$

and solved for  $m_c$  to obtain

$$m_c(m_2) = \frac{R(m_2) - m_b}{m_b R(m_2) + 1} \quad (17)$$

Equations (10) and (11) are each solved for  $Y_2$ , and then  $Y_2$  is eliminated by equating the resulting expressions:

$$Y_3 - (X_3 - X_2)m_b = y_2 + m_2(X_2 - x_2)$$

This equation is solved for  $X_2$  to yield

$$X_2(m_2) = \frac{m_2 x_2 - y_2 - m_b X_3 + Y_3}{m_2 - m_b} \quad (18)$$

This expression may be substituted back into equation (11) to obtain an expression for  $Y_2$  as a function of  $m_2$  only:

$$Y_2(m_2) = Y_3 - m_b[X_3 - X_2(m_2)] \quad (19)$$

Eliminating  $Y_1$  between equations (7) and (8) yields

$$Y_2 - m_c(X_2 - X_1) = y_0 + m_0(X_1 - x_0)$$

which can be solved for  $X_1$  and expressed as a function of  $m_2$  with substitutions from equations (17), (18), and (19):

$$X_1(m_2) = \frac{m_c(m_2)X_2(m_2) - Y_2(m_2) - m_0 x_0 + y_0}{m_c(m_2) - m_0} \quad (20)$$

This result is substituted back into equation (8) to obtain

$$Y_1(m_2) = y_0 + m_0[X_1(m_2) - x_0] \quad (21)$$

Equation (9) now becomes

$$m_1(m_2) = \frac{Y_1(m_2) - y_1}{X_1(m_2) - x_1} \quad (22)$$

Substituting from equations (17) and (22) into equation (5) yields

$$-2m_1(m_2)[1 - m_0 m_c(m_2)] + [m_0 + m_c(m_2)] \times \left\{ 1 - [m_1(m_2)]^2 \right\} = 0 \quad (23)$$

This equation is solved numerically by a forward seeker algorithm that finds the zeros of the function on the left side of equation (23). Once the root is found, we can find the remaining quantities by repeating the above substitutions with the known value of  $m_2$ . Thus,  $m_c$  is obtained from equation (17), and  $X_2, Y_2, X_1$ , and  $Y_1$  are obtained from equations (18) to (21).

To determine the next pair of points on the two reflectors,  $\theta_0$  is incremented. Then  $x_1, y_1, x_2$ , and  $y_2$  are incremented by specifying  $(X_1, Y_1)$  to be the midpoint of a segment on the subreflector and similarly for  $(X_2, Y_2)$  on the main reflector. Thus, for example,

$$x_{1,i} = x_{1,i-1} + 2(X_{1,i-1} - x_{1,i-1})$$

The procedure can then be repeated for the new value of  $\theta_0$ . Inasmuch as equation (23) is highly nonlinear and possesses multiple roots, some care must be exercised in setting the limits of the range of  $m_2$  over which the numerical algorithm seeks a solution. Fortunately, the limits are known to a close approximation because specifying even sizeable variations from a uniform intensity distribution or from a parallel-ray output beam does not result in large geometry variations from a conventional Cassegrain or Gregorian system.

### Computed Examples

Figure 3 shows a modified Cassegrain system for which the source distribution varies as  $\cos^8 \theta_0$  but the emitted beam is specified to have a uniform distribution. Figure 4 gives a similarly designed modification of a Gregorian system.

Figure 5 shows a modified Cassegrain system for which the slopes of the rays of the output beam are specified to increase gradually up to a value of 0.25:

$$m_3 = 0.25 \left( \frac{Y_3}{Y_{3,\max}} \right)^2$$

Figure 6 shows an offset system consisting of segments of a subreflector and a main reflector designed so that the emitted rays all have a slope of 0.25 relative to the system centerline. In such a system, the

cross-polarization phenomenon mentioned in the *Introduction* would exist.

### Concluding Remarks

A procedure has been described for designing dual-reflector antennas. The analysis was developed by taking each reflector to be the envelope of its tangent planes, so that the reflection condition is satisfied on each of these planes. The slopes of the emitted rays were specified rather than the phase distribution in the emitted beam.

Computed examples included variations from both Cassegrain and Gregorian systems. These examples include deviation from uniform source distribution and from the parallel-beam property of conventional systems.

NASA Langley Research Center  
Hampton, VA 23665-5225  
February 2, 1988

### References

1. Galindo, Victor: Design of Dual-Reflector Antennas With Arbitrary Phase and Amplitude Distributions. *IEEE Trans. Antennas & Propag.*, vol. 12, no. 4, July 1964, pp. 403-408.
2. Kinber, B. Ye.: On Two-Reflector Antennas. *Radio Eng. & Electron. Phys.*, no. 6, June 1962, pp. 914-921.

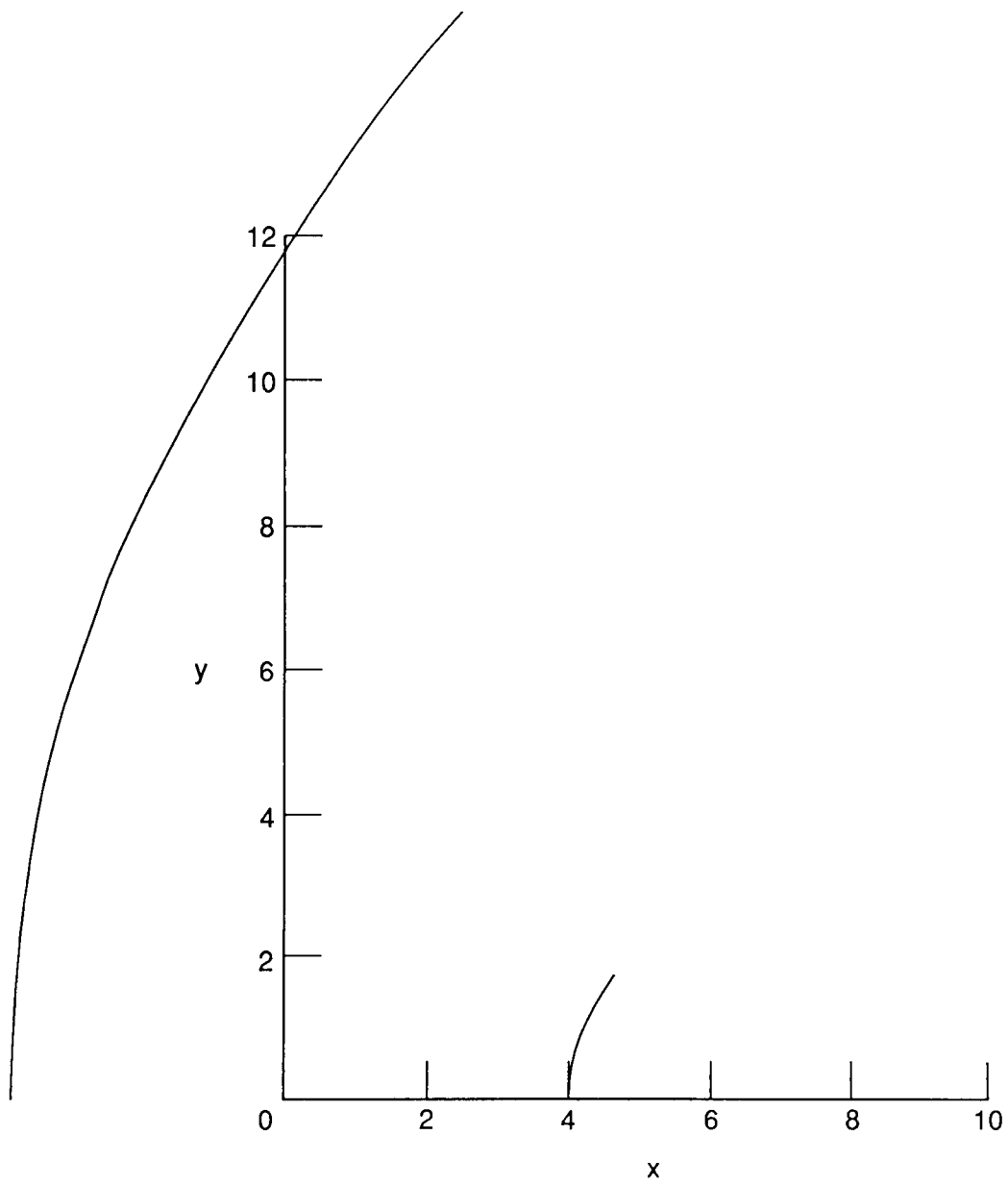


Figure 3. Modified Cassegrain system.



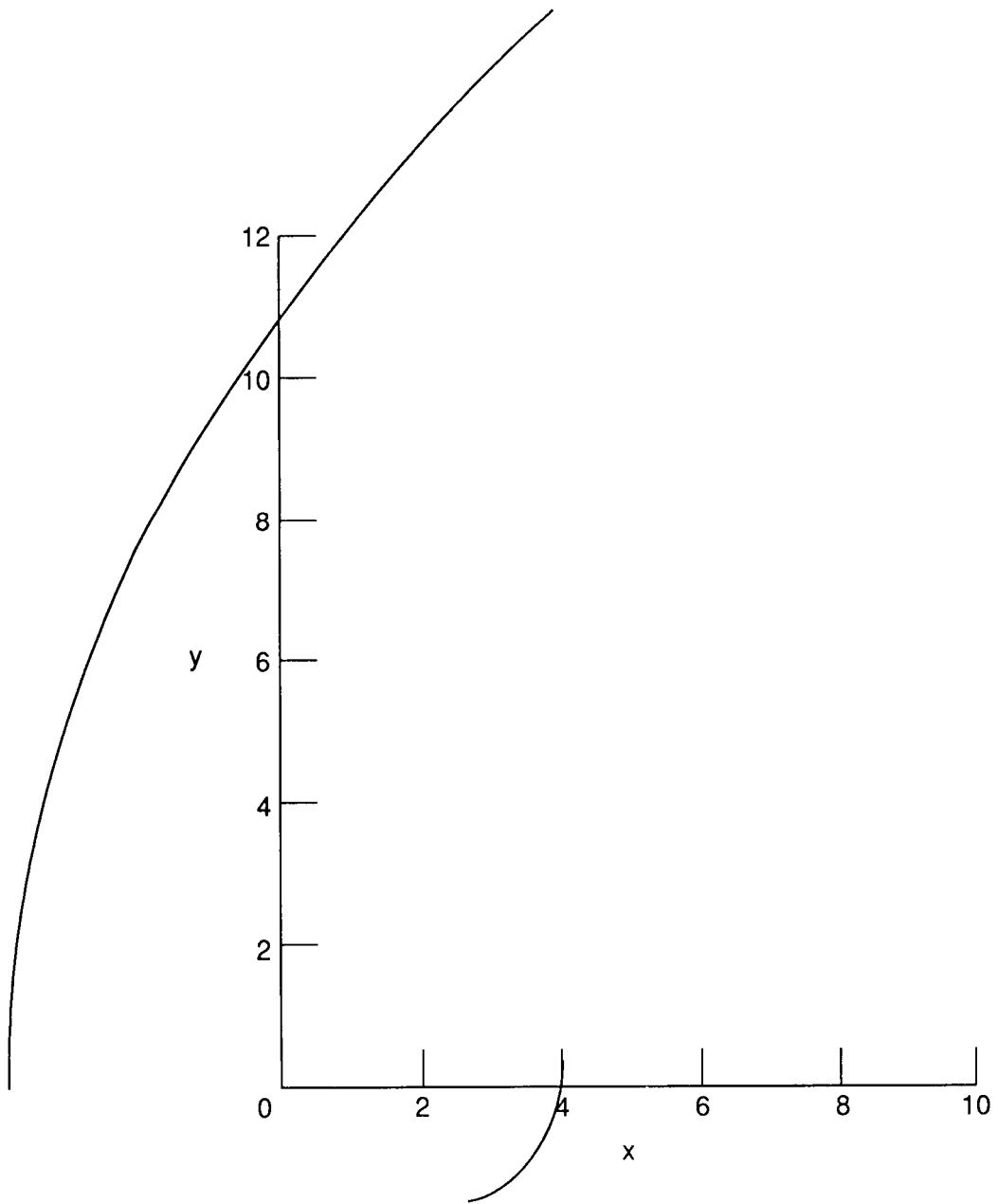


Figure 4. Modified Gregorian system.

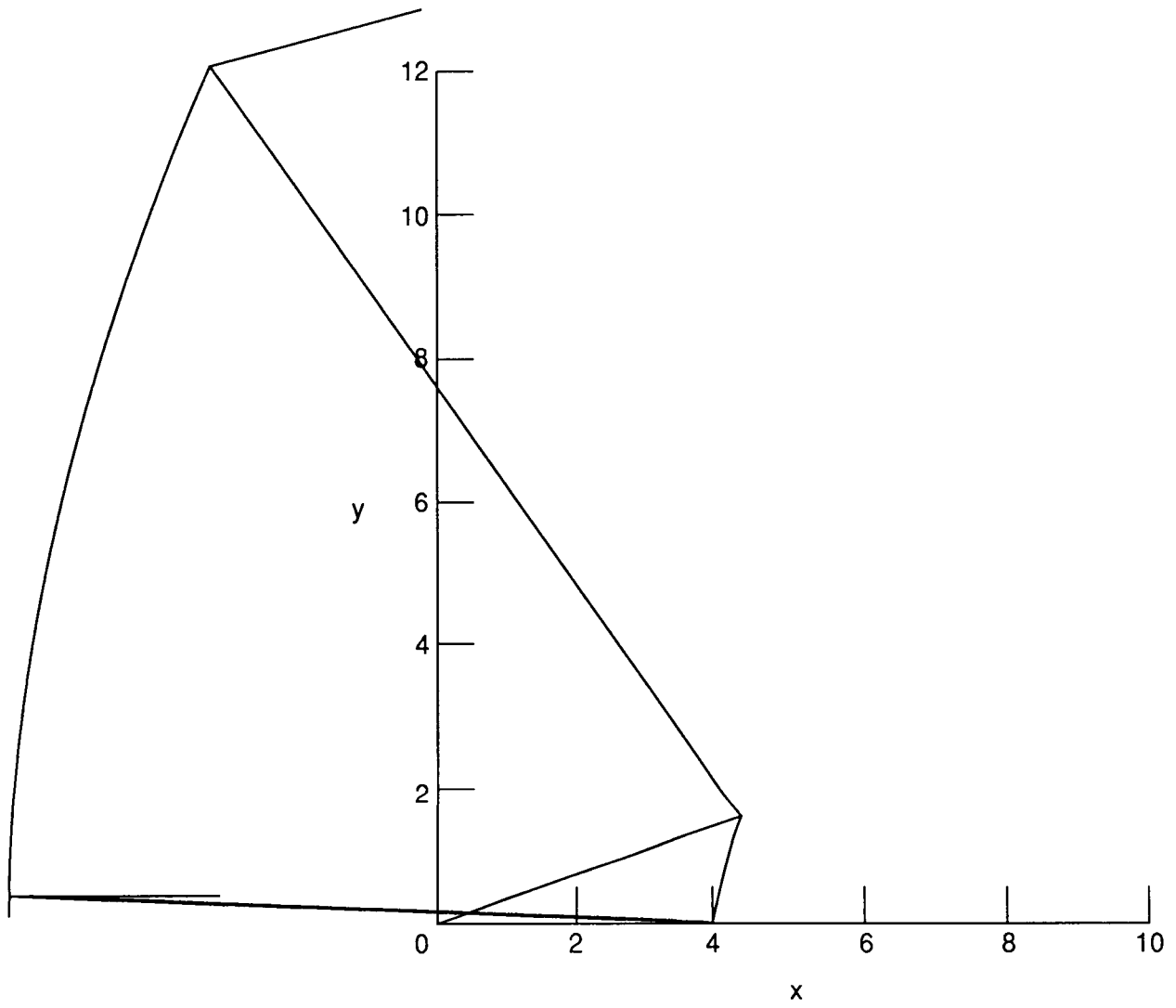


Figure 5. Modified Cassegrain system with ray slopes of output beam specified to increase to 0.25.

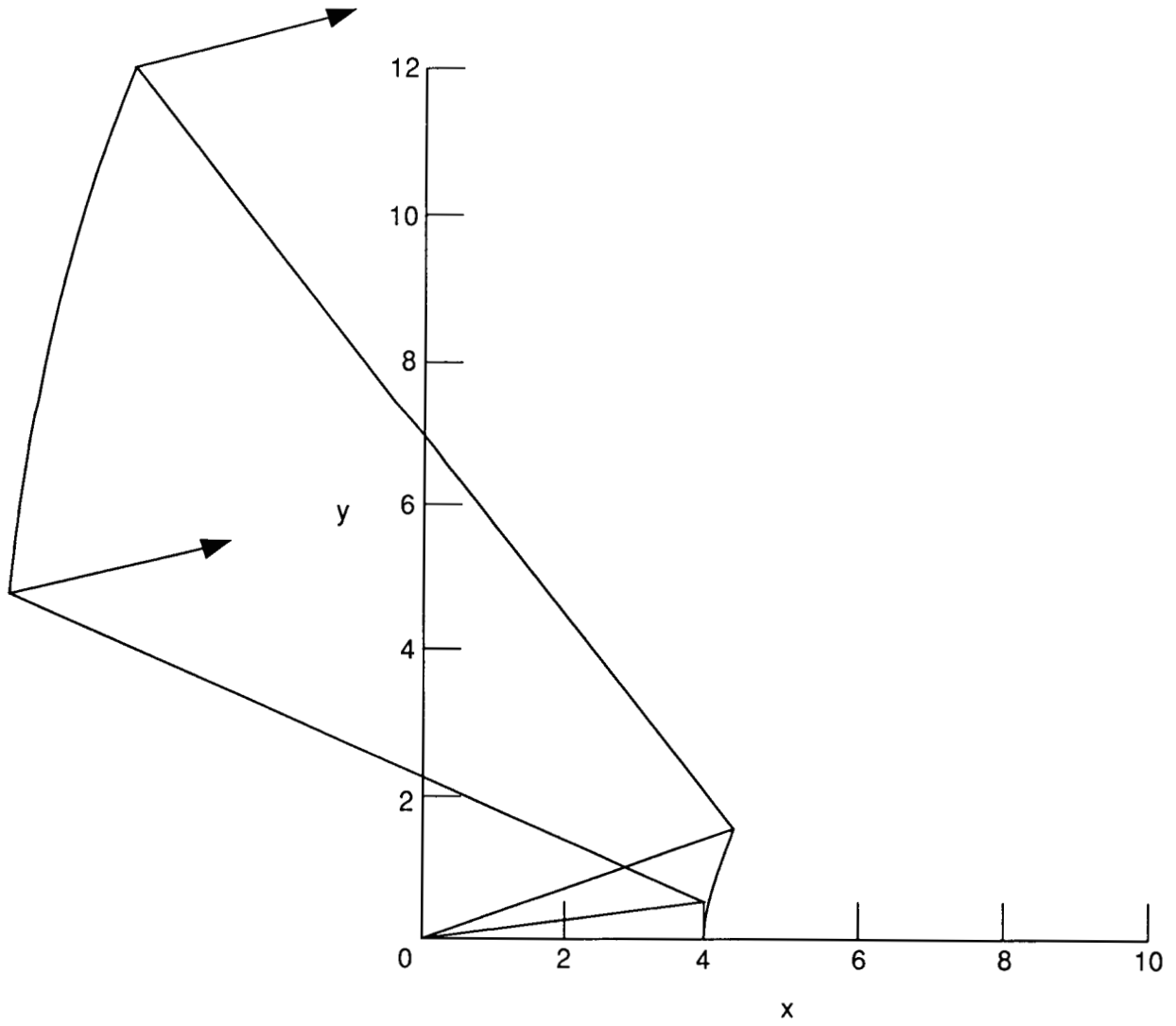


Figure 6. Cassegrain-type section designed to emit beam of rays at constant angle  $\theta_b \neq 0$ .



## Report Documentation Page

1. Report No. NASA TP-2797	2. Government Accession No.	3. Recipient's Catalog No.	
4. Title and Subtitle A Simplified Approach to Axisymmetric Dual-Reflector Antenna Design		5. Report Date March 1988	6. Performing Organization Code
		8. Performing Organization Report No. L-16392	
7. Author(s) Raymond L. Barger		10. Work Unit No. 505-61-71-04	
		11. Contract or Grant No.	
9. Performing Organization Name and Address NASA Langley Research Center Hampton, VA 23665-5225		13. Type of Report and Period Covered Technical Paper	
		14. Sponsoring Agency Code	
12. Sponsoring Agency Name and Address National Aeronautics and Space Administration Washington, DC 20546-0001			
15. Supplementary Notes			
16. Abstract A procedure is described for designing dual-reflector antennas. The analysis is developed by taking each reflector to be the envelope of its tangent planes. The slopes of the emitted rays were specified rather than the phase distribution in the emitted beam. Thus, both the output wave shape and the angular distribution of intensity can be specified. Computed examples include variations from both Cassegrain and Gregorian systems. These examples include deviation from uniform source distributions and from the parallel-beam property of conventional systems.			
17. Key Words (Suggested by Authors(s)) Dual-reflector antennas		18. Distribution Statement Unclassified—Unlimited	
		Subject Category 02	
19. Security Classif.(of this report) Unclassified	20. Security Classif.(of this page) Unclassified	21. No. of Pages 11	22. Price A02